Published in final edited form as:
Behav Brain Res. 2013 April 15; 243: 138–145. doi:10.1016/j.bbr.2012.12.062.

Heparan sulfate deficiency in autistic postmortem brain tissue from the subventricular zone of the lateral ventricles

Brandon L. Pearson[1,2,‡], **Michael J. Corley**[1,3,‡], **Amy Vasconcellos**[3], **D. Caroline Blanchard**[3,*], and **Robert J. Blanchard**[1]

[1]Department of Psychology, University of Hawaii, 2530 Dole Street, Honolulu, HI 96822, USA

[2]Department of Cell Biology and Physiology, University of North Carolina, 115 Mason Farm Road, Chapel Hill, NC 27599, USA

[3]Pacific Biosciences Research Institute, University of Hawaii, 1993 East-west Road, Honolulu, HI 96822, USA

Abstract

Abnormal cellular growth and organization have been characterized in postmortem tissue from brains of autistic individuals, suggestive of pathology in a critical neurogenic niche, the subventricular zone (SVZ) of the brain lateral ventricles (LV). We examined cellular organization, cell proliferation, and constituents of the extracellular matrix such as N-sulfated heparan sulfate (HS) and laminin (LAM) in postmortem brain tissue from the LV-SVZ of young to elderly individuals with autism ($n = 4$) and age-matched typically developing (TD) individuals ($n = 4$) using immunofluorescence techniques. Strong and systematic reductions in HS immunofluorescence were observed in the LV-SVZ of the TD individuals with increasing age. For young through mature, but not elderly, autistic pair members, HS was reduced compared to their matched TDs. Cellular proliferation (Ki67+) was higher in the autistic individual of the youngest age-matched pair. These preliminary data suggesting that HS may be reduced in young to mature autistic individuals are in agreement with previous findings from the BTBR T+tf/J mouse, an animal model of autism; from mice with genetic modifications reducing HS; and with genetic variants in HS-related genes in autism. They suggest that aberrant extracellular matrix glycosaminoglycan function localized to the subventricular zone of the lateral ventricles may be a biomarker for autism, and potentially involved in the etiology of the disorder.

Keywords

Autism; Postmortem; Subventricular zone; Extracellular matrix; Heparan sulfate; Neurogenesis

*Corresponding Author: D. Caroline Blanchard, Pacific Biosciences Research Center, 1993 East-West Rd., Honolulu, HI 96822, blanchar@hawaii.edu, phone (808) 956-8067, fax (808) 956-6984.
‡Authors Contributed Equally

Conflict of interest statement:
The authors declare no competing financial interests.

1. Introduction

Autism spectrum disorders (ASD) are a heterogeneous group of behaviorally defined, neurodevelopmental disorders [1]. Although there is strong evidence for genetic factors in ASD, it appears to be a polygenic condition [2, 3], and also responsive to a range of environmental/experiential events [4, 5]. Thus, its precise etiology is unknown [6]. A number of studies have reported abnormal cell growth and migration-related disturbances in postmortem tissue from brains of autistic individuals [7, 8], suggesting that the etiology of ASD involves aberrations in neurogenic processes in specific regions of the brain. The subventricular zone (SVZ) of the lateral ventricles (LV) is one of two neurogenic niches in the brain critical to neural proliferation, migration, and differentiation, both prenatally and into adulthood [9–11]. The unique structure and composition of the LV-SVZ regulates normal neurogenic functioning at various phases of development [10, 12]. Thus far, the cellular organization, proliferative cellular activity, and molecular compostion of the LV-SVZ region has not been examined in studies using postmortem tissue of autistic indivuals.

The extracellular glycosaminoglycan (GAG) heparan sulfate (HS) is a prominent and integral component of the LV-SVZ microenvironment [13]. The HS proteoglycan consists of a core protein, of which there are several families, to which GAG HS chains consisting of variably sulfated repeating disaccharide units are attached [14]. Both the core protein and the composition of the HS chains influence interactions with a wide variety of ligands, including growth factors and cytokines, resulting, in brain, in modulation of cell proliferation, differentiation, and migration [15, 16]. HS magnitude and composition are influenced by a variety of genes [17]; are responsive to environmental/experiential events such as oxidative stress [18], and modulate responsivity to inflammation [19]. They may change across development [20].

The purpose of the current study was to examine and characterize the LV-SVZ in postmortem tissue from individuals diagnosed with ASD. Specifically, the current study evaluated an hypothesis stemming from findings in a mouse model of autism [21, 22] that HS may be reduced in the human autistic LV-SVZ. This study examined postmortem tissue of autism-diagnosed individuals ($n = 4$) and age/sex matched typically developing (TD) controls ($n = 4$) from three areas of the LV-SVZ region using immunofluorescence methodology.

2. Methods

2.1. Brain tissue samples

Frozen postmortem brain tissue samples from male autism (ADI-R confirmed) cases and age/sex-matched controls were obtained from the Harvard Brain Tissue Resource Center and the NICHD Brain and Tissue Bank for Developmental Disorders through the Autism Tissue Program of Autism Speaks. Donor characteristics are presented in Table 1. Three frozen blocks per case were excised from the dorsal lateral ventricle wall including the anterior horn and body of the lateral ventricle. Blocks included portions of the medial caudate nucleus and body of the corpus callosum (Fig. 1a).

Tissue blocks (2.0 cm^3) from each case were sectioned on a cryostat (Leica, CM1850UV) perpendicular to and containing the ependymal, subependymal and parenchymal zones in the coronal plane at 10 μM. Tissue sections were mounted on Poly-L-lysine (1:5 Sigma-Aldrich) coated glass microscope slides (VWR superfrost) and stored at −20°C.

2.2. Immunohistochemistry

Slides were fixed in acetone (−20°C, 2 min) and rinsed in phosphate buffered saline (PBS) for 5 min. Wells were created on the slide with a hydrophobic barrier pen (Vector Labs, H-4000), tissue sections were permeabilized with Triton-X-100 (0.5%, 15 min, Fisher), blocked with a PBS gelatin blocking solution (0.2%, 10 min), labeled with antibodies, and cover slipped with a mounting medium containing 4′,6-diamidino-2-phenylindole (DAPI) nuclear marker (Vector Labs, H-1200).

Antibody specificity was tested by performing incubations in the absence of primary and/or secondary antibodies. Tissue sections, particularly those collected from older donors, exhibited lipofuscin-like autofluorescence [23] in the absence of antibodies. Two solutions (1% and 3%) of Sudan Black B (Sigma-Aldrich) [24] and a commercial reagent (Millipore, 2160) were tested on independent sections and assessed for autofluorescence blocking under 405nm, 488nm, and 546nm excitation on an Olympus Fluoview FV1000 laser scanning confocal microscope. Sudan black (1%) was the most effective at blocking non-specific autofluorescence and was used to treat all tissue sections.

For Ki67 protein and glial fibrillary acidic protein (GFAP) immunostaining, five randomly selected slides per case were incubated with anti-GFAP (1:1000, mouse IgG, Millipore) and anti-Ki67 (1:40, rabbit polyclonal, Millipore) for 24 hr, washed in PBS, blocked with a PBS gelatin blocking solution, and incubated with secondary antibodies Alexa Fluor 546 goat-anti rabbit IgG (1:400, Invitrogen) and Alexa Fluor 488 goat anti-mouse IgG (1:400, Invitrogen) for 40 min.

For heparan sulfate and laminin (LAM) immunostaining, fifteen slides per case, each distributed evenly throughout the antero-posterior extent of the blocks, were incubated with anti-heparan sulfate (1:400, mouse IgM, Seikagaku Corp, 10E4) and anti-Laminin (1:1000, rabbit IgG, Sigma-Aldrich) primary antibodies for 120 min, followed by washes in PBS and PBS gelatin blocking solution. Sections were then incubated with secondary antibodies Alexa Fluor 546 goat-anti rabbit IgG (1:400, Invitrogen) and Alexa Fluor 488 goat anti-mouse IgM (1:400, Invitrogen) for 40 min.

2.3. Microscopy and Image Processing

Researchers were blind to condition at all times during microscopy, image preparation, and quantification. Sections were imaged on an Olympus Fluoview FV1000 laser scanning microscope mounted on an Olympus IX81 inverted microscope at the Biological Electron Microscope Facility of the University of Hawaii. DAPI, AlexaFluor 488, and AlexaFluor 546 were excited sequentially at 405nm, 488nm, and 546nm respectively with blue diode, green HeNe, and red HeNe lasers. Microscopy images were exported as digital TIFF image files (1024X1024 pixels).

Images for DAPI, heparan sulfate, and laminin quantification (52–75 per case, non-overlapping fields) were acquired using a 20X UplanApo (0.70) optical objective with 2.0X digital zoom (fixed settings for laser power, high voltage, gain, and offset) along the entire dorsal-ventral extent of the ependymal layer (I) of the subventricular zone.

Z-stacks (1024X1024 pixels) for co-localization of Ki67/GFAP and heparan sulfate/laminin co-labeling were acquired with a UPLSAPO 60X oil-immersion lens (NA 1.35) at 1.0X and 2.0X zoom. Digital images were processed using Adobe Photoshop CS3 (Adobe Systems) and ImageJ (NIH). A minor levels adjustment was applied to all TIFF images in Adobe Photoshop.

2.4. Immunofluorescence Quantification

DAPI labeling was used to locate the layered cellular organization of the LV-SVZ and to quantify the width of the hypocellular layer (II) of the LV-SVZ. To assess the hypocellular width, coded TIFF images for each case were opened in ImageJ (NIH) software and five ROI measurements from the ependymal layer (1) to the astrocytic ribbon layer (III) of the LV-SVZ were averaged.

To assess cellular proliferation in the LV-SVZ, the mean number of Ki67+ cells was estimated by manually counting the number of Ki67+ cells in ten microscopic objective fields along the dorsal-ventral extent of the LV-SVZ for fifteen tissue sections per case.

To assess the localization and quantity of heparan sulfate and laminin immunofluorescence in different layers of the LV-SVZ, coded images were imported into ImageJ (NIH) software and converted into RGB stacks. The polygon selection tool was used to outline regions of interest (ROI) including the following areas of the LV-SVZ: a standardized 250 μM width area of the LV-SVZ extending from the ependymal layer (I) into layers (III) and (IV), the hypocellular layer (II) area of the LV-SVZ, and remaining layers (III) and (IV) combined of the LV-SVZ. This dimension (250 μM) was selected as a standard medio-lateral width because it includes the range of variable LV-SVZ widths demonstrated previously [25]. Large blood vessels and choroid plexus were omitted from fluorescence quantification measurements. Area, integrated density, and mean gray value were collected for the ROI as well as for three background areas per channel. Together, these were used to calculate corrected total fluorescence values [Integrated density − (area of selected zone × mean fluorescence of background images)] according to previously published methods for each image [26].

2.5. Statistical Analysis

Mean corrected total fluorescence values for the 250μM, hypocellular region as well as hypocellular layer width and Ki67+ cell counts were compared with two-way analyses of variance (ANOVA) with condition (Autism vs. Control) and Age as main factors. When main effects or interactions were found, Bonferroni post hoc comparisons were performed to assess significant differences between conditions at each age group. Unpaired t-tests were used to compare mean fluorescence and cell count values across all ages. A probability of $p < .05$ was adopted as the level of statistical significance.

3. Results

3.1. DAPI localization of the LV-SVZ in autistic and TD postmortem tissue

DAPI nuclear labeling guided the localization of the layered human LV-SVZ for autism-diagnosed and control tissue sections (Fig. 1b). Autism-diagnosed tissue did not differ from TD samples in the characteristic layered organization of the human LV-SVZ. In coronal sections, the area bordering the lateral wall of the lateral ventricles consisted of a one to two cell DAPI+ cell layer corresponding to the ependymal layer (I). Adjacent to ependymal layer was the hypocellular layer (II), which was mostly devoid of DAPI+ cells except for a few displaced ependymal cells. DAPI+ cells were present in the layer (III) that has been characterized to consist of a continuous band of astrocytes and the layer (IV) that blended into the adjoining parenchyma [10, 12]. Since DAPI staining reveals a defined hypocellular layer (II) largely devoid of positive cells, we investigated whether the hypocellular gap width differed between autism and control samples (Fig. 1b, c). The hypocellular gap width did not significantly differ between autism and TD samples; however, the hypocellular gap width was larger for older tissue samples compared to younger samples [$t(298) = 9.76$, $p < .0001$] (Fig. 1b, c).

3.2. Ki67 immunofluorescence

The mean number of Ki67+ proliferating cells were increased in tissue from the autistic member of the 5–6 year-old pair [$p<.001$] reflecting an increase in actively mitotic cells, with no notable differences between pair members thereafter (Fig. 2a). Ki67+ proliferating cells were observed on the ependymal wall, within the hypocellular layer (II), and within layers (III) and (IV) of the LV-SVZ (Fig. 2b, c). We examined the co-localization of Ki67 and GFAP and observed Ki67+/GFAP+ cells near the ependymal wall of the youngest autistic sample (Fig. 2d), suggestive of a distinct type of proliferating cell with possible stem cell properties [10].

3.3. Examination of extracellular matrix component HS

HS immunofluorescence was more localized to the hypocellular layer (II) region of the LV-SVZ for autism and typically developing control cases [$t(584) = 6.67$, $p<.0001$] (Fig. 3a). When the entire section, from the ventricle wall to a standard distance of 250 μm was analyzed, HS immunofluorescence in tissue from typically developing control individuals declined systematically with increasing age (Fig. 3b). This age-related decline in HS immunofluorescence was less marked in tissue from autistic individuals and HS levels were sharply lower than those of the paired TD-control value at each of the youngest age-matched pairs [p<.001] (Fig. 3b, c, d). In the 60-year old pair, HS immunofluorescence levels were very low for both the autistic and the TD members of the pair (Fig 3e, f). Over all 4 pairs, this autism – TD difference was significant [$F(1,289) = 46.11$, $p<.0001$]. This consistent decrease in HS with age for the TD group reflected age-related changes localized to the hypocellular layer (Fig. 4a, b, c).

3.4. Examination of basement membrane component LAM immunofluorescence

The concentration of LAM (amount per unit area) was significantly higher in the hypocellular layer (II) than in layers (III) and (IV) [$t(584) = 13.22$, $p<.0001$] (Fig. 4a), although LAM-positive capillaries were present in the latter; supporting the functional localization of LAM to the basement membrane of the LV-SVZ [27]. LAM fluorescence in tissue from autistic individuals was different from that of the TD pair-members [$F(1,383) = 8.27$, $p=.004$] (Fig. 4b). However, these differences were not consistent across condition or age.

3.5. HS/LAM and LAM/GFAP co-localization

In the hypocellular zone of autism-diagnosed and TD cases, the extracellular matrix consisted of LAM-dense zones corresponding to fractone or fractone-like basal lamina structures [28] surrounded by GFAP+ astrocytic processes extending from the characteristic astrocytic ribbon layer in the human LV-SVZ [12] (Fig. 6a). In the hypocellular layer (II) area of samples from young, young-adult, and middle-aged autism and TD individuals, HS frequently co-localized with LAM (Fig. 6b).

4. Discussion

In this first report of findings from examination of postmortem tissue from the LV-SVZ region of autistic and TD individuals, HS in the LV-SVZ was reduced in tissue from brains of younger autistic individuals, relative to TD controls. Tissue from the 60-year old autistic individual did not display reduced HS relative to its TD pair-member. However, HS levels declined sharply and systematically with increasing age for the 4 TD individuals, consistent with previous findings in both human and rodent brain tissue [29–31] and HS was extremely low in the 60-year old TD pair member, with levels converging for the two members of this pair. Thus, the lack of a substantial autistic-TD difference in this oldest pair appears to reflect this decline in HS with age, in the LV-SVZ for TD individuals.

Increased cellular proliferation (Ki67+) was also noted in tissue from the youngest autistic individual, only, with no pair differences thereafter. This age-related increased proliferation is interesting in the context of a well-documented enhancement of prefrontal cortical volume in autistic children between about 1–2 and 10 years of age, with subsequent normalization [7, 32]. Sanai et al. have reported that in young human brains a substantial offshoot of the LV-SVZ rostral migratory stream is directed at the prefrontal cortex [33]. However, additional research needs to determine whether alternations in the LV-SVZ underlie the cortical volume differences reported in autism. That this increase in Ki67+ cells was found in conjunction with reduced HS levels is compatible with reports suggesting that some HS configurations may be associated with reductions, rather than increases in neurogenesis [34].

In the current study, the monoclonal antibody for HS recognized enriched N- sulfated motifs of the disaccharide chain [35]. HS chains differ in a host of posttranslational modifications, including sulfation, to produce what has been called “the most information dense molecules found in nature” [36]. Thus, these differences in all but the oldest autistic-TD pair could reflect a specific reduction in N- sulfated HS in autistic individuals, rather than a general HS reduction. Given the many roles that HS proteoglycans play in the development of virtually every body organ, the relative lack of robust anatomical or physiological differences for autistic individuals may suggest HS changes that are specific to the brain, or to the LV-SVZ, or that involve only some particular components of the “heparanome” [37]. Brain infusions of the closely related glycosaminoglycan heparin sulfate have been reported to modulate learning and memory in an age-dependent manner [38, 39]; suggesting that manipulation of endogenous GAGs or administration of exogenous GAGs may modulate cognitive processes and behavior and might provide a potential treatment approach for some of the behavioral aberrations associated with ASD.

It is notable that both autistic children, and BTBR T+tf/J mouse model of autism, show substantially reduced levels of sulfates in peripheral tissues [40–46]; potentially interesting in terms of the possibility of a specific reduction in N-sulfated HS, and raising the possibility that the HS differences measured here reflect under-sulfation (ie.[47]), rather than a general reduction in HS. In addition, findings of increased cell proliferation only in LV-SVZ tissue from the 5-year-old autistic individual suggests that HS composition may vary with age. Clearly, additional work on the composition of HS and HS proteoglycans in the LV-SVZ in autistic individuals is needed to clarify these questions, and to suggest particular downstream mechanisms that might be altered because of these HS changes and their interactions with growth and guidance factors in the LV- SVZ [15]. In the hypocellular layer (II) area, HS frequently co-localized with LAM suggesting that the latter may be an important basement membrane substrate for HS activity. However, LAM levels, while consistently different between members of age-pairs, did not show a consistent direction of difference for tissue from autistic individuals.

Post-mortem histopathological examination results were available for two of the four autism-diagnosed individuals in this study. Both showed altered neural anatomy and cellular proliferation. The five-year-old autistic individual showed cortical dysplasia in parietal and occipital lobes and flocculonodular dysplasia in the cerebellum (ATP Neuropath Report). The sixty year old displayed frontal and entorhinal cortex focal dysplasia as well as cellular and morphological disturbances of the dentate gyrus and cerebellum and region-dependent increases and decreases in neuronal volume and density (ATP Neuropath Report). These brain changes are similar to those found in previously analyzed brain tissue: Indeed the 60-year old autistic individual was part of the cohort reported by Wegiel et al. [8] and suggest that HS interactions with growth and guidance factors may be involved. Nonetheless, given that histopathological examinations are not available for the other samples, any specific

connection between N-sulfated HS levels and development of the brain in autistic individuals remains speculative.

The responsivity of HS to potentially relevant genetic and environmental effects [19] provides an additional rationale for attempts to determine if, and how, perturbations of these dynamic systems are involved in autism. Insofar as HS, or other mechanisms in the LV-SVZ, are factors in the development of autism, the search for genetic signatures related to autism might be particularly appropriate in this area. In particular, the concept of genetic "vulnerability" to environmental/experiential events implied in an interactive view of the etiology of autism might be examined specifically in the context of altered LV-SVZ gene expression related to HS and the growth and guidance factors that it influences.

Finally, the hypothesis that HS in the LV-SVZ may be altered in autistic individuals was based on, and reflects, reports of reduced HS in the LV-SVZ in BTBR T+tf/J mice, which show autism-relevant changes in each of the 3 symptom-clusters by which autism is defined [21, 22, 48]. The hypothesis also agrees with findings that conditional *Ext1* knockout mice, lacking HS postnatally, show a deficit in social behaviors and an increase in stereotyped behaviors [49]; and with reports of genetic conditions impacting HS in autistic individuals [50]. A substantial proportion of the 25+ genes regulating HS [51] have been associated with autism: In particular, genes regulating HS synthesis (*EXT1*, *EXT2*: [52, 53]), and disaccharide residue sulfation/deacetylation (*HS3ST5*, *HS3ST6*, *NDST4*: [52, 54, 55]) have shown autism related variants. BTBR T+tf/J mice also show a variety of physiological differences from more social strains such as the C57BL/6J, including neuroanatomic abnormalities; changes in neurodevelopmental proteins; enhanced systemic glucocorticoids; and changes in immune systems that provide potential links to findings reported in autistic individuals (reviewed in [48]). To this burgeoning evidence that the BTBR T+tf/J mouse can serve as a particularly appropriate and specific animal model for autism, the present study adds predictive validity that a particular, area-localized change in an important brain molecule, noted for the BTBR T+tf/J mouse, is also found in autistic individuals. This reduction in HS is potentially related to a number of the neuroanatomical [56] and immune system [57] changes noted in autism. The BTBR T+tf/J mouse, as well as other mouse strains with alterations of this system, may provide a highly appropriate model for examining changes in the heparanome and their effects on the brain and behavior.

Our finding that n-sulfated HS in the LV-SVZ appears to be reduced in brains of all but elderly autistic individuals, compared to TD age- and sex-matched pair members, suggests that HS may contribute to the aberrations in brain development and behavior that are seen in autism. These findings suggest the value of detailed analyses of HS content and composition in the LV-SVZ, as well as determinations of potential changes in gene expression in this area, for autistic vs. TD individuals at different ages.

Acknowledgments

Funded by NIH R01 MH081845 to RJB. We are grateful for the contributions of Autism Tissue Program of Autism Speaks, the Harvard Brain Tissue Resource Center, which is supported in part by PHS grant number R24 MH 068855, and the NICHD Brain and Tissue Bank. We are especially grateful to the families who donated specimens.

References

1. Betancur C. Etiological heterogeneity in autism spectrum disorders: more than 100 genetic and genomic disorders and still counting. Brain research. 2011; 1380:42–77. [PubMed: 21129364]
2. Geschwind DH. Genetics of autism spectrum disorders. Trends in cognitive sciences. 2011; 15:409–16. [PubMed: 21855394]

3. Glessner JT, Wang K, Cai G, Korvatska O, Kim CE, Wood S, et al. Autism genome-wide copy number variation reveals ubiquitin and neuronal genes. Nature. 2009; 459:569–73. [PubMed: 19404257]
4. Depino AM. Peripheral and central inflammation in autism spectrum disorders. Molecular and cellular neurosciences. 2012
5. Landrigan PJ. What causes autism? Exploring the environmental contribution. Current opinion in pediatrics. 2010; 22:219–25. [PubMed: 20087185]
6. Lord CE. Autism: from research to practice. The American psychologist. 2010; 65:815–26. [PubMed: 21058793]
7. Courchesne E, Mouton PR, Calhoun ME, Semendeferi K, Ahrens-Barbeau C, Hallet MJ, et al. Neuron number and size in prefrontal cortex of children with autism. JAMA: the journal of the American Medical Association. 2011; 306:2001–10. [PubMed: 22068992]
8. Wegiel J, Kuchna I, Nowicki K, Imaki H, Marchi E, Ma SY, et al. The neuropathology of autism: defects of neurogenesis and neuronal migration, and dysplastic changes. Acta neuropathologica. 2010; 119:755–70. [PubMed: 20198484]
9. Alvarez-Buylla A, Lim DA. For the long run: maintaining germinal niches in the adult brain. Neuron. 2004; 41:683–6. [PubMed: 15003168]
10. Quinones-Hinojosa A, Sanai N, Soriano-Navarro M, Gonzalez-Perez O, Mirzadeh Z, Gil-Perotin S, et al. Cellular composition and cytoarchitecture of the adult human subventricular zone: a niche of neural stem cells. The Journal of comparative neurology. 2006; 494:415–34. [PubMed: 16320258]
11. Riquelme PA, Drapeau E, Doetsch F. Brain micro-ecologies: neural stem cell niches in the adult mammalian brain. Philosophical transactions of the Royal Society of London Series B, Biological sciences. 2008; 363:123–37.
12. Sanai N, Tramontin AD, Quinones-Hinojosa A, Barbaro NM, Gupta N, Kunwar S, et al. Unique astrocyte ribbon in adult human brain contains neural stem cells but lacks chain migration. Nature. 2004; 427:740–4. [PubMed: 14973487]
13. Mercier F, Arikawa-Hirasawa E. Heparan sulfate niche for cell proliferation in the adult brain. Neuroscience letters. 2012; 510:67–72. [PubMed: 22230891]
14. Sarrazin S, Lamanna WC, Esko JD. Heparan sulfate proteoglycans. Cold Spring Harbor perspectives in biology. 2011:3.
15. Kreuger J, Spillmann D, Li JP, Lindahl U. Interactions between heparan sulfate and proteins: the concept of specificity. The Journal of cell biology. 2006; 174:323–7. [PubMed: 16880267]
16. Yamaguchi Y. Heparan sulfate proteoglycans in the nervous system: their diverse roles in neurogenesis, axon guidance, and synaptogenesis. Seminars in cell & developmental biology. 2001; 12:99–106. [PubMed: 11292375]
17. Yoneda A, Lendorf ME, Couchman JR, Multhaupt HA. Breast and ovarian cancers: a survey and possible roles for the cell surface heparan sulfate proteoglycans. The journal of histochemistry and cytochemistry: official journal of the Histochemistry Society. 2012; 60:9–21. [PubMed: 22205677]
18. Kennett EC, Chuang CY, Degendorfer G, Whitelock JM, Davies MJ. Mechanisms and consequences of oxidative damage to extracellular matrix. Biochemical Society transactions. 2011; 39:1279–87. [PubMed: 21936802]
19. Axelsson J, Xu D, Kang BN, Nussbacher JK, Handel TM, Ley K, et al. Inactivation of heparan sulfate 2-O-sulfotransferase accentuates neutrophil infiltration during acute inflammation in mice. Blood. 2012; 120:1742–51. [PubMed: 22791291]
20. Leberfarb EY, Rykova VI, Kolosova NG, Dymshits GM. Age-related changes in proteoglycan composition in rat brain. Bulletin of experimental biology and medicine. 2008; 146:797–9. [PubMed: 19513387]
21. Blanchard DC, Defensor EB, Meyza KZ, Pobbe RL, Pearson BL, Bolivar VJ, et al. BTBR T+tf/J mice: autism-relevant behaviors and reduced fractone-associated heparan sulfate. Neuroscience and biobehavioral reviews. 2012; 36:285–96. [PubMed: 21741402]

22. Meyza KZ, Blanchard DC, Pearson BL, Pobbe RL, Blanchard RJ. Fractone-associated N-sulfated heparan sulfate shows reduced quantity in BTBR T+tf/J mice: a strong model of autism. Behavioural brain research. 2012; 228:247–53. [PubMed: 22101175]
23. Schnell SA, Staines WA, Wessendorf MW. Reduction of lipofuscin-like autofluorescence in fluorescently labeled tissue. The journal of histochemistry and cytochemistry: official journal of the Histochemistry Society. 1999; 47:719–30. [PubMed: 10330448]
24. Oliveira VC, Carrara RC, Simoes DL, Saggioro FP, Carlotti CG Jr, Covas DT, et al. Sudan Black B treatment reduces autofluorescence and improves resolution of in situ hybridization specific fluorescent signals of brain sections. Histology and histopathology. 2010; 25:1017–24. [PubMed: 20552552]
25. van den Berge SA, Middeldorp J, Zhang CE, Curtis MA, Leonard BW, Mastroeni D, et al. Longterm quiescent cells in the aged human subventricular neurogenic system specifically express GFAP-delta. Aging cell. 2010; 9:313–26. [PubMed: 20121722]
26. Burgess A, Vigneron S, Brioudes E, Labbe JC, Lorca T, Castro A. Loss of human Greatwall results in G2 arrest and multiple mitotic defects due to deregulation of the cyclin B-Cdc2/PP2A balance. Proceedings of the National Academy of Sciences of the United States of America. 2010; 107:12564–9. [PubMed: 20538976]
27. Mercier F, Kitasako JT, Hatton GI. Anatomy of the brain neurogenic zones revisited: fractones and the fibroblast/macrophage network. The Journal of comparative neurology. 2002; 451:170–88. [PubMed: 12209835]
28. Shen Q, Wang Y, Kokovay E, Lin G, Chuang SM, Goderie SK, et al. Adult SVZ stem cells lie in a vascular niche: a quantitative analysis of niche cell-cell interactions. Cell stem cell. 2008; 3:289–300. [PubMed: 18786416]
29. Jenkins HG, Bachelard HS. Developmental and age-related changes in rat brain glycosaminoglycans. Journal of neurochemistry. 1988; 51:1634–40. [PubMed: 3139839]
30. Komosinska-Vassev K, Olczyk P, Winsz-Szczotka K, Klimek K, Olczyk K. Plasma biomarkers of oxidative and AGE-mediated damage of proteins and glycosaminoglycans during healthy ageing: a possible association with ECM metabolism. Mechanisms of ageing and development. 2012; 133:538–48. [PubMed: 22813851]
31. Rykova VI, Leberfarb EY, Stefanova NA, Shevelev OB, Dymshits GM, Kolosova NG. Brain proteoglycans in postnatal development and during behavior decline in senescence-accelerated OXYS rats. Advances in gerontology = Uspekhi gerontologii/Rossiiskaia akademiia nauk, Gerontologicheskoe obshchestvo. 2011; 24:234–43.
32. Vaccarino FM, Grigorenko EL, Smith KM, Stevens HE. Regulation of cerebral cortical size and neuron number by fibroblast growth factors: implications for autism. Journal of autism and developmental disorders. 2009; 39:511–20. [PubMed: 18850329]
33. Sanai N, Nguyen T, Ihrie RA, Mirzadeh Z, Tsai HH, Wong M, et al. Corridors of migrating neurons in the human brain and their decline during infancy. Nature. 2011; 478:382–6. [PubMed: 21964341]
34. Sasaki N, Hirano T, Kobayashi K, Toyoda M, Miyakawa Y, Okita H, et al. Chemical inhibition of sulfation accelerates neural differentiation of mouse embryonic stem cells and human induced pluripotent stem cells. Biochemical and biophysical research communications. 2010; 401:480–6. [PubMed: 20875394]
35. David G, Bai XM, Van der Schueren B, Cassiman JJ, Van den Berghe H. Developmental changes in heparan sulfate expression: in situ detection with mAbs. The Journal of cell biology. 1992; 119:961–75. [PubMed: 1385449]
36. Li L, Ly M, Linhardt RJ. Proteoglycan sequence. Molecular bio Systems. 2012; 8:1613–25.
37. Turnbull J, Powell A, Guimond S. Heparan sulfate: decoding a dynamic multifunctional cell regulator. Trends in cell biology. 2001; 11:75–82. [PubMed: 11166215]
38. Jezek K, Schulz D, De Souza Silva MA, Muller HW, Huston JP, Hasenohrl RU. Effects of chronic intraventricular infusion of heparin glycosaminoglycan on learning and brain acetylcholine parameters in aged rats. Behavioural brain research. 2003; 147:115–23. [PubMed: 14659577]

39. De Souza Silva MA, Jezek K, Weth K, Muller HW, Huston JP, Brandao ML, et al. Facilitation of learning and modulation of frontal cortex acetylcholine by ventral pallidal injection of heparin glucosaminoglycan. Neuroscience. 2002; 113:529–35. [PubMed: 12150773]
40. Adams JB, Audhya T, McDonough-Means S, Rubin RA, Quig D, Geis E, et al. Nutritional and metabolic status of children with autism vs. neurotypical children, and the association with autism severity. Nutrition & metabolism. 2011; 8:34. [PubMed: 21651783]
41. Alberti A, Pirrone P, Elia M, Waring RH, Romano C. Sulphation deficit in “low-functioning” autistic children: a pilot study. Biological psychiatry. 1999; 46:420–4. [PubMed: 10435209]
42. Corley MJ, Meyza KZ, Blanchard DC, Blanchard RJ. Reduced sulfate plasma concentrations in the BTBR T+tf/J mouse model of autism. Physiology & behavior. 2012
43. Geier DA, Kern JK, Garver CR, Adams JB, Audhya T, Geier MR. A prospective study of transsulfuration biomarkers in autistic disorders. Neurochemical research. 2009; 34:386–93. [PubMed: 18612812]
44. Waring R, Klovrza L. Sulphur metabolism in autism. Journal of Nutritional and Environmental Medicine. 2000; 10:25–32.
45. Waring R, Naidu S, Skjeldal O, Klovrza L, Reichelt KL. Sulphur anion metabolism in Rett syndrome patients: A pilot study. Journal of Pediatric Neurology. 2006; 4:233–7.
46. Waring R, Ngong J, Klovrza L, Green S, Sharp H. Biochemical parameters in autistic children. Developmental Brain Dysfunction. 1997; 10:40–3.
47. Karus M, Samtleben S, Busse C, Tsai T, Dietzel ID, Faissner A, et al. Normal sulfation levels regulate spinal cord neural precursor cell proliferation and differentiation. Neural development. 2012; 7:20. [PubMed: 22681904]
48. Meyza KZ, Defensor EB, Jensen AL, Corley MJ, Pearson BL, Pobbe RL, et al. The BTBR T(+)tf/J mouse model for autism spectrum disorders-in search of biomarkers. Behavioural brain research. 2012
49. Irie F, Badie-Mahdavi H, Yamaguchi Y. Autism-like socio-communicative deficits and stereotypies in mice lacking heparan sulfate. Proceedings of the National Academy of Sciences of the United States of America. 2012; 109:5052–6. [PubMed: 22411800]
50. Ishikawa-Brush Y, Powell JF, Bolton P, Miller AP, Francis F, Willard HF, et al. Autism and multiple exostoses associated with an X;8 translocation occurring within the GRPR gene and 3′ to the SDC2 gene. Human molecular genetics. 1997; 6:1241–50. [PubMed: 9259269]
51. Bishop JR, Schuksz M, Esko JD. Heparan sulphate proteoglycans fine-tune mammalian physiology. Nature. 2007; 446:1030–7. [PubMed: 17460664]
52. Iossifov I, Ronemus M, Levy D, Wang Z, Hakker I, Rosenbaum J, et al. De novo gene disruptions in children on the autistic spectrum. Neuron. 2012; 74:285–99. [PubMed: 22542183]
53. Li H, Yamagata T, Mori M, Momoi MY. Association of autism in two patients with hereditary multiple exostoses caused by novel deletion mutations of EXT1. Journal of human genetics. 2002; 47:262–5. [PubMed: 12032595]
54. O’Roak BJ, Vives L, Girirajan S, Karakoc E, Krumm N, Coe BP, et al. Sporadic autism exomes reveal a highly interconnected protein network of de novo mutations. Nature. 2012; 485:246–50. [PubMed: 22495309]
55. Wang K, Zhang H, Ma D, Bucan M, Glessner JT, Abrahams BS, et al. Common genetic variants on 5p14.1 associate with autism spectrum disorders. Nature. 2009; 459:528–33. [PubMed: 19404256]
56. Amaral DG, Schumann CM, Nordahl CW. Neuroanatomy of autism. Trends in neurosciences. 2008; 31:137–45. [PubMed: 18258309]
57. Onore C, Careaga M, Ashwood P. The role of immune dysfunction in the pathophysiology of autism. Brain, behavior, and immunity. 2012; 26:383–92.

Highlights

- We examine the neurogenic subventricular zone (SVZ) in postmortem autism tissue.
- Decreased heparan sulfate immunofluorescence in autism SVZ tissue.
- Increased cellular proliferation in the 5 yr old autism-diagnosed SVZ tissue.
- Aberrant extracellular matrix function in the SVZ may be a biomarker for autism.

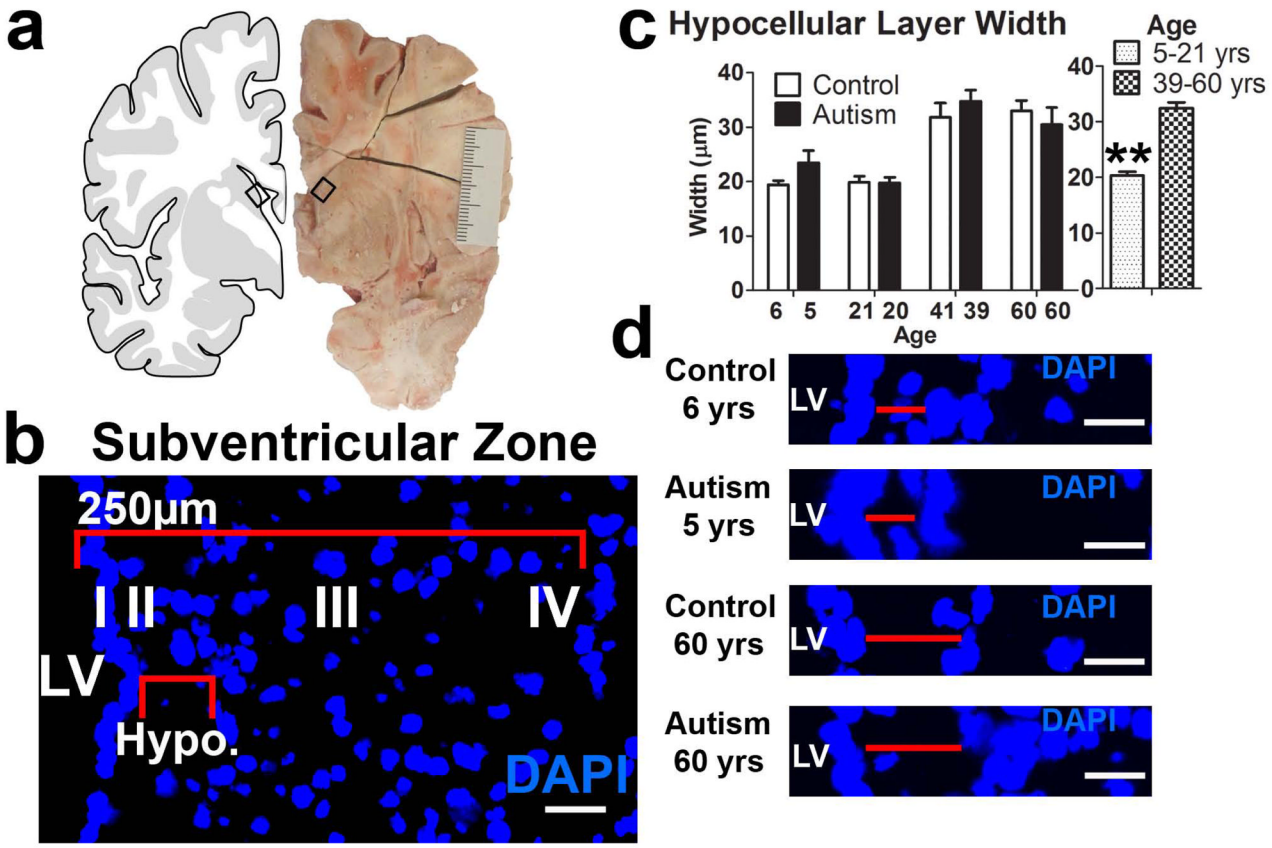

Figure 1.

Cellular organization in the human subventricular zone of the lateral ventricles. (a) Representative excised tissue block from a coronal section containing the LV-SVZ (b) Layered morphology of human LV-SVZ. I–IV label ependymal, hypocellular gap [Hypo.], astrocytic ribbon and transitional zone layers, respectively. (c) Hypocellular layer width similar across conditions, but significantly increased in tissue derived from 39 to 60 year olds compared to 5 to 21 year olds (mean+sem, **P<.01). (d) Hypocellular gap width measurement of young and old autism and typically developing control samples. Scale bars: 30 µm. LV- lateral ventricle. AU- arbitrary units.

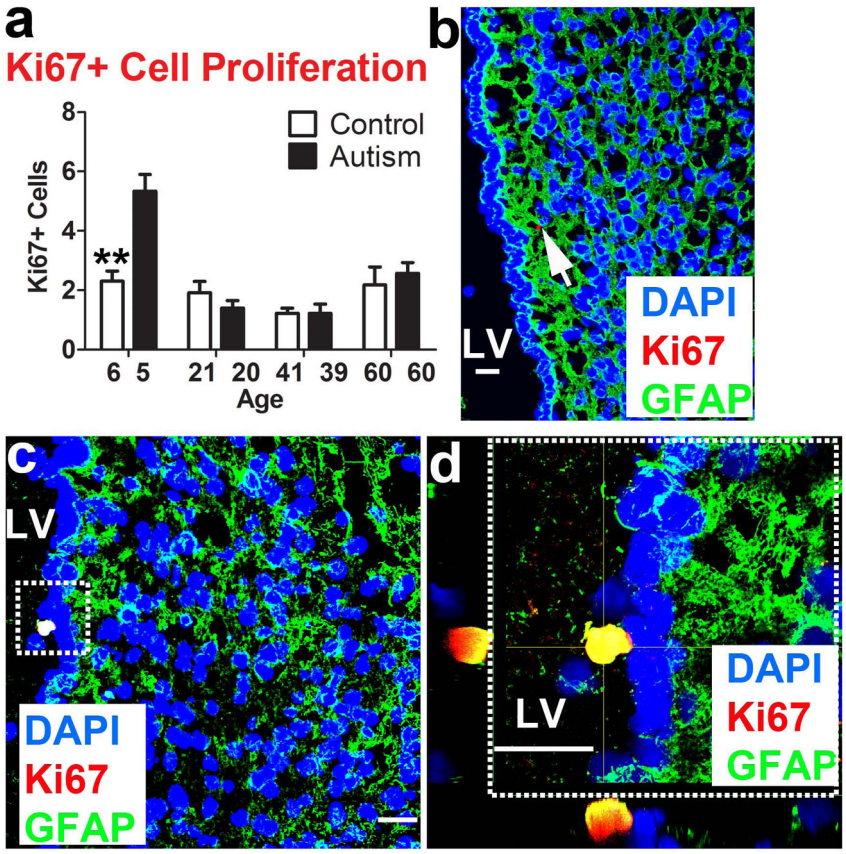

Figure 2.

Increased proliferation in the LV-SVZ in youngest autism case (AN08873). (a) Autism-diagnosed 5 year old sample shows increased number of proliferating cells compared to age-matched control sample (mean+sem, **P<.01). (b) Ki67+ cells (arrow) were present in the hypocellular layer of 5 yr old autism case and contained GFAP+ astrocytic processes. (c) Additionally, Ki67+ cells were viewed on the ependymal wall and (d) dashed box denotes higher-magnification z-stack showing co-localization of Ki67 and GFAP in tissue from the 5 yr old autism case. Scale bars: 30 μm. LV- lateral ventricle. Scale bars: 30 μm. LV- lateral ventricle. AU- arbitrary units.

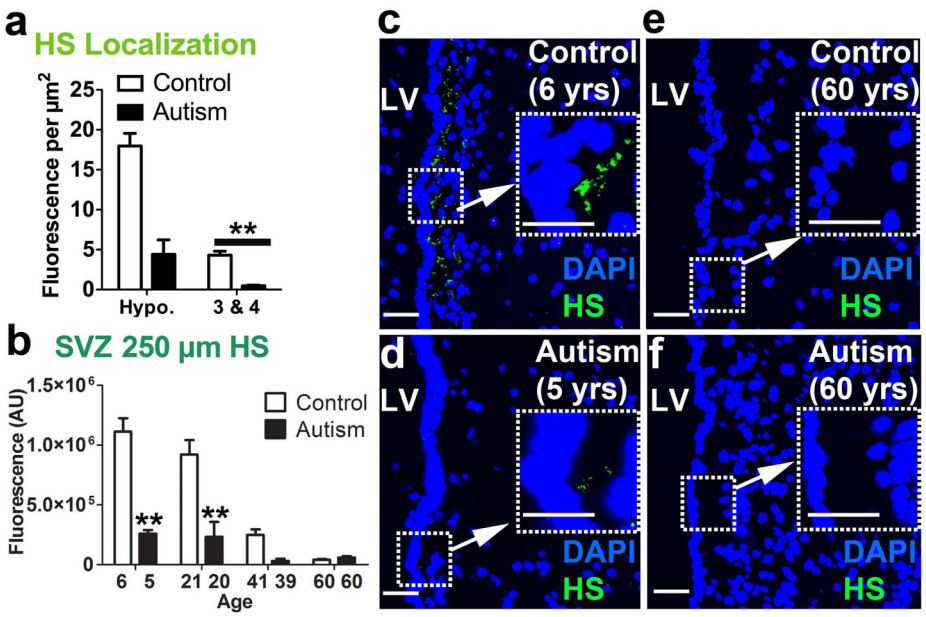

Figure 3.

HS is reduced in the LV-SVZ of autistic individuals and decreases by age in typically developing controls. (a) HS is localized to the hypocellular region compared to layers 3 & 4 (mean+sem, **P<.01). (b) 250 μm into the LV-SVZ, HS is decreased overall in autism-diagnosed samples compared to controls; young (5–6) and young adult (20–21) autism-diagnosed samples significantly lower than TD controls (mean+sem, **P<.01). (c, d, e, f) HS is decreased in young (5–6) but not older (60) autism-diagnosed samples. Scale bars: 30 μm. LV- lateral ventricle. AU- arbitrary units.

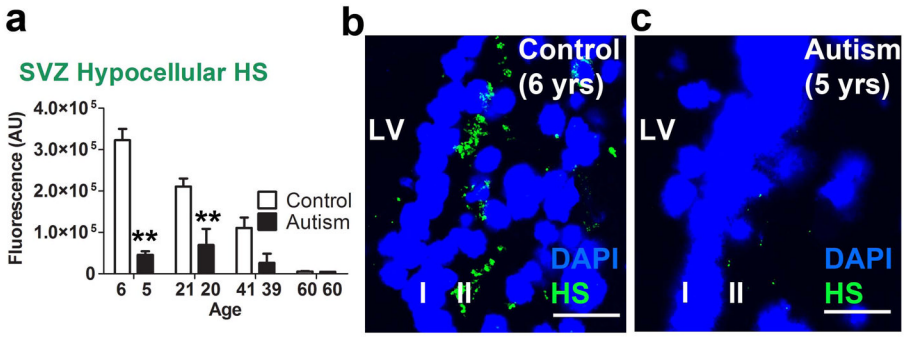

Figure 4.

HS in the hypocellular layer of the LV-SVZ is decreased in autistic individuals and decreases by age in typically developing controls (a) HS immunoreactivity is elevated lateral to ventricular wall in young and young adult typically developing controls but not autism-diagnosed samples (mean+sem, **P<.01). (b, c) HS is enriched in hypocellular layer (layer II) of the young TD control, but not ASD sample. Scale bars: 30 μm. LV- lateral ventricle. AU-arbitrary units.

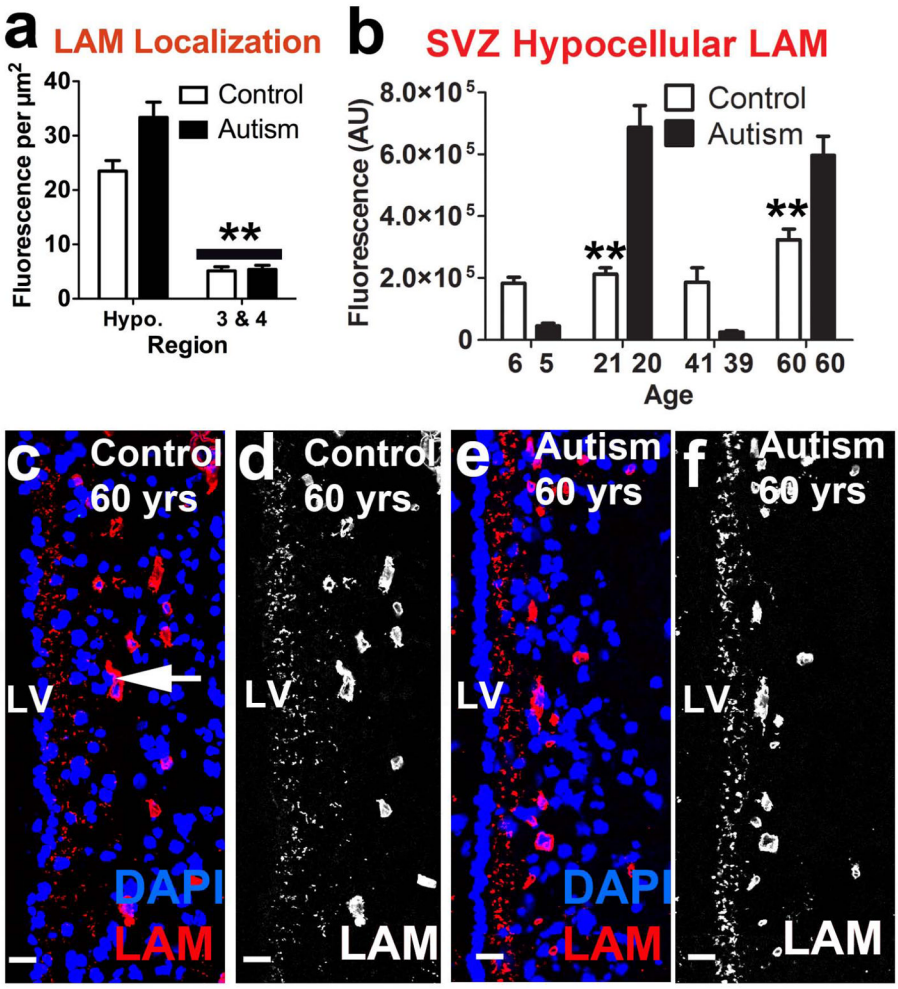

Figure 5.

Laminin is abundant in the hypocellular layer. (a) LAM is enriched in the hypocellular layer across conditions compared to layers 3 and 4 of the SVZ. (b) Autism samples show complex age-specific changes in LAM immunoreactivity in the LV-SVZ. (c, d, e, f) Confocal micrographs demonstrating abundant LAM glycoprotein in the hypocellular layer and capillaries (arrow) of 60 yr old control and autism samples. Scale bars: 30 μm. LV- lateral ventricle. AU- arbitrary units.

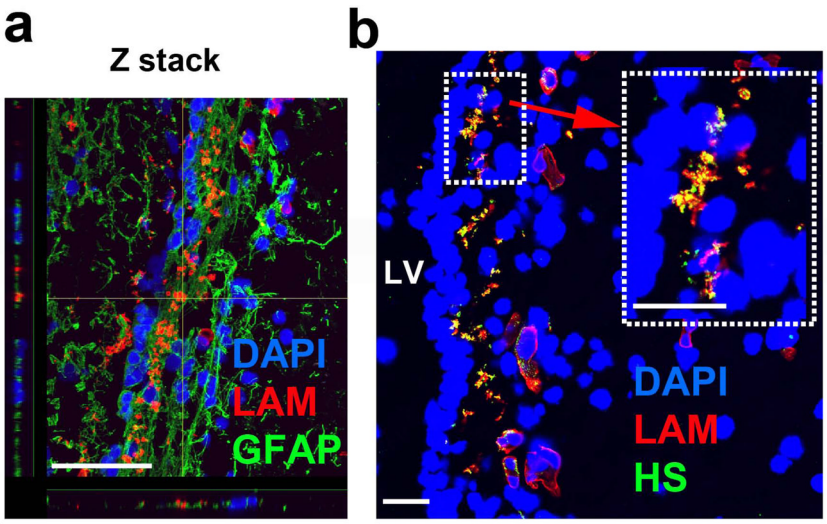

Figure 6.

Astrocytic processes interact with laminin and heparan sulfate is localized to basement membrane laminin in the hypocellular layer. (a) Maximal projection Z stack displays proximal association of hypocellular LAM and astrocytic processes in the hypocellular, subependymal layer. (b) LAM and HS co-labeling in the extracellular matrix of hypocellular layer. Scale bars: 30 μm. LV- lateral ventricle. AU- arbitrary units.

Table 1

Postmortem brain tissue case characteristics.

Autism (ADI-R Diagnosed)					***Typically-Developing Control***				
ID	**Age (years)**	**PMI (h)***	**Cause of Death**	**Brain Weight (g)**	**ID**	**Age (years)**	**PMI (h)#**	**Cause of Death**	**Brain Weight (g)**
AN08873	5 *	25.5	Drowning	1560	UMB5408	6.86	16	Drowning	1320
AN00764	20	23.7	Auto Accident	1144	UMB1405	21	13	Drowning	1440
AN06420	39	13.95	Cardiac Tamponade	1520	AN01410	41	27.17	N/A	N/A
AN09714	60.11 *	26.5	Pancreatic Cancer	1210	AN10723	60	24.23	Heart Attack	1340
MEAN	*31*	*22.41*				*32*	*20.1*		

*Neuropathological Report Available,

#PMI: Postmortem Interval